

UNCLASSIFIED

SECURITY CLASSIFICATION OF THIS PAGE

REPORT DOCUMENTATION PAGE

AD-A208 723

1b RESTRICTIVE MARKINGS

3 DISTRIBUTION/AVAILABILITY OF REPORT

Approved for public release; distribution is unlimited.

4 PERFORMING ORGANIZATION REPORT NUMBER(S)

5 MONITORING ORGANIZATION REPORT NUMBER(S)

6a NAME OF PERFORMING ORGANIZATION

Naval Weapons Center

6b OFFICE SYMBOL
(If applicable)

7a NAME OF MONITORING ORGANIZATION

6c ADDRESS (City, State, and ZIP Code)

China Lake, CA 93555

7b ADDRESS (City, State, and ZIP Code)

8a NAME OF FUNDING/SPONSORING
ORGANIZATION

Office of Naval Research

8b OFFICE SYMBOL
(If applicable)

9. PROCUREMENT INSTRUMENT IDENTIFICATION NUMBER

8c ADDRESS (City, State, and ZIP Code)

800 N. Quincy
Arlington, VA 22217

10. SOURCE OF FUNDING NUMBERS

PROGRAM
ELEMENT NOPROJECT
NOTASK
NOWORK UNIT
ACCESSION NO.

11 TITLE (Include Security Classification)

Crystal Chemistry, Synthesis, and Characterization of Infrared Optical Materials

12 PERSONAL AUTHOR(S)

D. O. Kipp, C. K. Lowe-Ma, and T. A. Vanderah

13a TYPE OF REPORT

13b TIME COVERED
FROM TO

14. DATE OF REPORT (Year, Month, Day)

1988

15 PAGE COUNT

16 SUPPLEMENTARY NOTATION

Presented at the Materials Research Society Meeting, San Diego, 24-28 April 1989

17 COSATI CODES

FIELD GROUP SUB-GROUP

18 SUBJECT TERMS (Continue on reverse if necessary and identify by block number)

19 ABSTRACT (Continue on reverse if necessary and identify by block number)

DTIC
ELECTE
MAY 31 1989
S H D

20 DISTRIBUTION/AVAILABILITY OF ABSTRACT

☒ UNCLASSIFIED/UNLIMITED ☐ SAME AS RPT ☐ DTIC USERS21 ABSTRACT SECURITY CLASSIFICATION
UNCLASSIFIED

22a NAME OF RESPONSIBLE INDIVIDUAL

T. A. Vanderah

22b TELEPHONE (Include Area Code)

619-939-1654

22c OFFICE SYMBOL

3854

DD FORM 1473, 84 MAR

83 APR edition may be used until exhausted
All other editions are obsolete

SECURITY CLASSIFICATION OF THIS PAGE

U.S. Government Printing Office: 1985-507-047

UNCLASSIFIED

89 5 31 050

CRYSTAL CHEMISTRY, SYNTHESIS, AND CHARACTERIZATION OF INFRARED OPTICAL MATERIALS

D.O. KIPP, C.K. LOWE-MA, AND T.A. VANDERAH
Chemistry Division (Code 3854), Research Department
Naval Weapons Center, China Lake, CA 93555

ABSTRACT

Non-oxide inorganic compounds such as sulfides, phosphides, and mixed-anion sulfide-phosphides are of interest as possible infrared window materials. Our research on the solid state chemistry and structure-property relationships of these materials includes the directed synthesis of new compounds as well as the study of compounds that have been reported in the literature but which have been incompletely characterized for this application.

The present work includes investigations of three ternary sulfide systems: ZnGa_2S_4 , AlIn_2S_4 , ($A = \text{Ca, Sr, Ba}$), and CaY_2S_4 . Samples were prepared in polycrystalline form and/or as crystals. New compounds were obtained in our studies of the CaIn_2S_4 , SrIn_2S_4 , and CaY_2S_4 systems. Compounds were characterized by X-ray diffraction, elemental analysis, FTIR, and thermogravimetric analysis.

INTRODUCTION

Compounds that are candidates for use as long-wavelength (8-12 μm) infrared-transmitting window materials must have a certain set of chemical and physical properties [1-6]. The low fundamental vibrational frequencies that result in the desired optical transparency are favored by weak chemical bonds (high coordination numbers) and heavy constituent atoms. This requirement eliminates all oxides and other strong ceramic materials such as BN and Si_3N_4 , whose strong chemical bonds among relatively light atoms cause fundamental absorptions in the long-wavelength infrared region. However, these strong chemical bonds also result in desirable properties such as chemical inertness, high mechanical strength, and low thermal expansion. Therefore, in the search for new materials for long-wavelength windows, an inherent trade-off situation exists: the chemical characteristics that will tend to give the best structural-ceramic properties will always tend to degrade the optical properties since the stronger the chemical bonding, the higher the vibrational frequencies. Our compromise approach in seeking and designing new compounds has been to achieve long-wavelength IR transparency by the use of highly charged, heavy atoms in three-dimensional crystal structures that feature intermediate cation coordination numbers of 5-6. Compounds that fulfill this structural-chemical requirement are predicted to retain satisfactory mechanical properties and chemical inertness. To minimize absorption, compounds should also be non-paramagnetic insulators or large bandgap semiconductors.

The ternary sulfide ZnGa_2S_4 was first reported in 1955 by Hahn, et al [7]. This compound is of interest in second-phase toughening studies of ZnS [8] and exhibits long-wavelength infrared transparency comparable to that of ZnS [9]. Colorless ZnGa_2S_4 crystals with tetrahedral-like morphology are easily obtained by iodine transport [10], and studies of mechanical and electrical properties have been reported [11,12]. Hahn, et al [7], postulated that the structure of this compound was that of an ordered defect sphalerite, the ordering of the defects and the two different cations giving rise to two possible structural arrangements, A and B, illustrated in Fig. 1. These two arrangements cannot be distinguished by X-ray powder diffraction. Despite the ease of growing crystals of ZnGa_2S_4 , a full single-crystal structure determination has not, to our knowledge, been reported. To confirm the predicted structure and determine the cation/defect ordering pattern, a complete X-ray crystal structure determination was undertaken.

The first report of CaIn_2S_4 was in 1950 [13]. The authors claimed that X-ray powder diffraction data indicated a normal spinel structure ($a = 10.77 \text{ \AA}$) for this compound. This structure is chemically unreasonable for CaIn_2S_4 , as Ca^{2+} would be tetrahedrally coordinated by

sulfur. In addition, In_2S_3 has a spinel-like structure. It is likely, therefore, that this report of CaIn_2S_4 is erroneous, and that the reported diffraction data correspond to In_2S_3 . A compound with a similar ternary formula, $\text{Ca}_{3.1}\text{In}_{6.6}\text{S}_{13}$, [14a] has been synthesized as yellow whiskers in iodine transport reactions. A single-crystal X-ray diffraction investigation [14b] found a monoclinic structure with indium octahedrally coordinated and calcium in tri-capped trigonal prismatic coordination: space group C2/m , $a = 37.63(1)$, $b = 3.8358(9)$, $c = 13.713(3)$ Å, $\beta = 91.65(1)^\circ$.

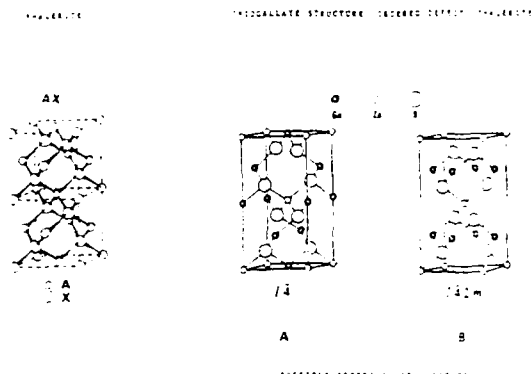


Fig. 1. ZnGa_2S_4 Structure.

SrIn_2S_4 and BaIn_2S_4 were first reported in 1974 [15]. These pink-colored compounds were prepared from the elements by iodine transport and found to be isostructural by X-ray powder diffraction. The powder patterns were indexed on a pseudo-orthorhombic cell ($a = 10.548$, $b = 6.510$, $c = 10.439$ Å for SrIn_2S_4 and $a = 10.840$, $b = 6.556$, $c = 10.885$ Å for BaIn_2S_4), although a larger orthorhombic superlattice was suggested. A single-crystal X-ray diffraction study of BaIn_2S_4 [16] found the barium in square antiprismatic sites and the indium in tetrahedral sites. An orthorhombic unit cell was indicated with each axis doubled relative to the first report (space group Fddd , $a = 21.824(6)$, $b = 21.670(6)$, $c = 13.125(4)$ Å). Our investigation of these ternary indium sulfide systems was undertaken to confirm the reported structures and elucidate any structural interrelationships, and to characterize their properties pertinent for use as optical materials.

All studies to date on the ternary yttrium sulfide CaY_2S_4 have been on polycrystalline samples. The compound was first reported in 1961 by Flahaut [17], but its exact crystal structure is still unknown. All models that have been proposed are derived from the structure of $\text{VIII}(\text{CaVI})\text{Fe}_2\text{O}_4$. This structure features "double rutile-like" edge-sharing chains of distorted FeO_6 octahedra. Different double-chains are connected by vertex-linking to form a relatively open, three-dimensional framework. Channels in the framework feature numerous different sites with a variety of possible coordination numbers for the larger Ca cation, thus allowing considerable structural variety. The earliest X-ray powder diffraction studies of CaY_2S_4 [17] indicated a large orthorhombic unit cell, given in Table I, column A, that was consistent with the Yb_2S_4 structure and therefore 7-coordinate Ca. In 1967, a high-temperature form of CaY_2S_4 [18], quenchable from 1100°C , was reported with the orthorhombic cell given in Table I, column B. Interestingly, the unit cell obtained for the high-temperature form indicated an overall volume decrease resulting from contraction of two of the cell parameters. This form was reported as having the MnY_2S_4 structure, in which all cations are 6-coordinate and 0.5 mol each of Ca and Y apparently disorder across the channel and framework cation sites. In 1981, a third form of CaY_2S_4 was reported as having a monoclinic unit cell [19], given in Table I, column C. Raman and infrared spectroscopic studies of CaY_2S_4 powder [20] indicated an onset of infrared transmission loss near 400 cm^{-1} ($25\text{ }\mu\text{m}$), with the highest fundamental vibrational frequency occurring at 315 cm^{-1} ($31\text{ }\mu\text{m}$). Since this infrared transparency looked very promising compared to the presently available long-wavelength material, ZnS , a study of CaY_2S_4 was undertaken to further determine its structure and properties.

Accession For	
NTIS GRA&I	<input checked="" type="checkbox"/>
DTIC TAB	<input type="checkbox"/>
Unannounced	<input type="checkbox"/>
Justification	
By	
Distribution/	
Availability Codes	
Dist	Avail and/or Special
A-1	

Table I. Unit Cells that Have Been Reported for CaY_2S_4 :

A - orthorhombic Yb_2S_4 structure, $\text{VI}(\text{Ca})\text{VI}(\text{Y})_2\text{S}_4$ [18]		
B - high-temperature orthorhombic MnY_2S_4 structure, $\text{VI}(\text{Ca})\text{VI}(\text{Y})_2\text{S}_4$ [18]		
C - monoclinic, structure unknown [19]		
A	B	C
$a = 12.98 \text{ \AA}$	$a = 12.90 \text{ \AA}$	$a = 12.88 \text{ \AA}$
$b = 13.11 \text{ \AA}$	$b = 13.17 \text{ \AA}$	$b = 13.04 \text{ \AA}$
$c = 3.88 \text{ \AA}$	$c = 3.87 \text{ \AA}$	$c = 4.02 \text{ \AA}$
		$\beta = 93.48^\circ$

EXPERIMENTAL METHODS

Sample Characterization

X-ray powder diffraction data were obtained with a Scintag PAD V diffractometer and/or by Gandolfi or Debye-Scherrer camera methods. Cell parameters were calculated from powder diffractometer data using a least-squares refinement program. For single crystals, unit cells and lattice symmetries were obtained with a Nicolet R3 diffractometer. Elemental compositions were estimated by electron microscopy using the SEM/EDX method (AMRAY 1400, TRACOR TN2000 analyzer). Accurate elemental compositions of crystals thought to be new compounds were determined by ICP emission analysis (ICAP/OES, Perkin Elmer 6500). Oxidative stability was measured by thermogravimetric analysis (TGA) under flowing oxygen (Du Pont 1090). Infrared spectra were obtained in diffuse reflectance and transmission modes using a Nicolet 60 SX FTIR spectrophotometer.

Sample Preparation

ZnGa_2S_4 crystals were readily obtained with the CVT method using iodine as the transport agent [10,12] for polycrystalline ZnGa_2S_4 , which had been previously prepared by reacting the binary sulfides at 900°C in vacuo. The temperature gradient was $50\text{--}75^\circ\text{C}$ (silica ampule 1.0 cm I.D. x 19 cm long) with the charge end at 960°C . SEM/EDX analysis was consistent with the expected composition and the X-ray powder diffraction pattern of the colorless tetrahedral-like crystals agreed with that reported [21] for tetragonal ZnGa_2S_4 ; $a = 5.27$, $c = 10.4 \text{ \AA}$ [7].

Crystals of CaIn_2S_4 , $\text{Ca}_{1.2}\text{In}_{1.9}\text{S}_4$, and $\text{Sr}_{0.9}\text{In}_{2.1}\text{S}_4$ were grown in similar manners from eutectic halide fluxes. CaS and In_2S_3 were pre-reacted in a graphite crucible in an evacuated silica ampule at 1100°C for 6 days before use in the Ca-In-S flux growth experiments. According to X-ray powder diffraction, the yellow-brown polycrystalline product contained CaS , In_2S_3 , and a phase later identified as CaIn_2S_4 . The binary sulfide powders were used as the charge in the crystal growth of $\text{Sr}_{0.9}\text{In}_{2.1}\text{S}_4$. Mixtures of charge and flux (CaCl_2/KCl 75:25 mol% for Ca-In-S systems; SrCl_2/KCl 45:55 mol% for the Sr-In-S system) were reacted in graphite crucibles in evacuated silica ampules. The reaction mixtures were heated to 1100°C , held for 3 days, cooled at $1.0\text{--}1.5^\circ\text{C/h}$ to 500°C , and then cooled to room temperature in 1 day. The crystals were removed from the flux by soaking with distilled water. Yields of approximately 15% for the calcium compounds and 2% for the strontium compound were obtained. The crystals were present as mats of whiskers distributed throughout the flux. Many of the whisker-like crystals of these three compounds could be seen to be agglomerations of smaller parallel whiskers under an optical microscope. The formulas given above were determined by ICP.

BaIn_2S_4 was prepared in polycrystalline form from the binary sulfides. The reactants were heated in a graphite crucible in an evacuated silica ampule at 1050°C for 6 days.

Polycrystalline CaY_2S_4 was prepared by reacting stoichiometric quantities of the binary sulfides in a carbon crucible in an evacuated silica ampule for 18 d at 960°C , followed by slow-cooling. X-ray diffraction indicated complete reaction. Crystals were grown using a 0.24 $\text{CaCl}_2/0.76 \text{ KCl}$ eutectic mixture as the flux. The flux-to-charge ratio was approximately 10:1 by weight; the charge composition was half CaY_2S_4 powder and half a stoichiometric mixture of the binary sulfides. The reaction was heated in a carbon crucible enclosed in an evacuated silica ampule at 1010°C for 3 weeks, and then slow-cooled at $2^\circ/\text{h}$ to some unknown temperature at which point the furnace burned out and rapid cooling ensued. The flux was removed by soaking in water for several days. Golden light-brown whiskers up to 1 cm in length were recovered from the silica ampule wall. SEM/EDX analysis indicated a composition consistent with CaY_2S_4 , and the X-ray powder pattern of the whiskers matched that of the CaY_2S_4 powder. More numerous in yield were transparent, orange polyhedral crystals displaying cubic-like morphology up to 1 mm on an edge that were found on the ampule walls as well as within the flux. These crystals displayed a simple cubic, CaS -like X-ray powder diffraction pattern. SEM/EDX analyses of six crystals indicated similar compositions with substantial yttrium contents. ICP emission analysis of the crystals indicated the formula $\text{Ca}_{0.625}\text{Y}_{0.250}\text{S}$ or $\text{Ca}_5\text{Y}_2\text{S}_8$.

RESULTS

ZnGa_2S_4

The location of mirror planes on preliminary X-ray precession alignment photographs relative to the external morphology of three tetrahedral-like crystals of ZnGa_2S_4 clearly showed that the crystals were, in fact, tetragonal disphenoids. The two proposed structural arrangements A or B (Fig. 1) belong to two different Laue groups, $4/m$ for A and $4/mmm$ for B. Laue photographs exhibited Laue symmetry $4/mmm$, suggesting the defect/cation ordering arrangement of B. This conclusion is in agreement with the Laue symmetry observed by White [22] who also concluded that ZnGa_2S_4 would have structure B. However, White mentioned that Raman spectra exhibited both sharp and broad bands possibly suggesting some disordering.

A colorless, transparent crystal of 0.22 mm on an edge was used for the crystal structure determination. A constrained least-squares fit of twenty-five computer-centered reflections yielded unit cell parameters $a = 5.274(1)$, $c = 10.407(2)$ Å, $V = 289.5(1)$ Å³. Intensity data were obtained at room temperature from 4° to 70° 2θ (Mo K α) for octants hkl and $h\bar{k}l$. No violations of the I-centering and no additional systematic absences were observed. After numerical absorption corrections, equivalent data were satisfactorily merged in $I4_2m$ to give 360 unique, observed data. The large observation-to-parameter ratio (approximately 20:1) resulted in many false minima during least-squares refinement. The refinement finally converged to an R-factor = 0.043.

Refinement of the single-crystal data confirms that the structure is, in general, as shown in B of Fig. 1. However, this refinement also indicates some slight disorder of the cations and vacancies. The vacancy site appears to contain about 1.8% "Zn". The Zn site appears to contain about 5.6% more "Zn" than expected with the Ga and S site occupations held fixed. Some disordering of the cations and vacancies is not surprising in view of the very rapid rate of crystal growth that we observed and this would explain the earlier Raman results observed by White [22].

AlIn_2S_4 Systems, A = Ca, Sr, Ba

CaIn_2S_4 was obtained as yellow whiskers up to ca. 3 mm in length. However, when the charge:flux mass ratio was increased from 1:4 to 1:7, (increasing the overall Ca:In ratio in the reaction mixture) bronze-colored whiskers of stoichiometry $\text{Ca}_{1.2}\text{In}_{1.9}\text{S}_4$ resulted.

The unit cell for a yellow whisker of CaIn_2S_4 was obtained by single-crystal methods and indicated a C-centered monoclinic cell. Refinement of powder data from crushed crystals (Fig. 2, middle) gave cell parameters $a = 37.628(4)$, $b = 3.8361(8)$, $c = 13.722(1)$ Å, and $\beta = 91.66(1)^\circ$. This unit cell agrees with that reported in the single-crystal study of

$\text{Ca}_{3.1}\text{In}_{6.6}\text{S}_{13}$ [14b]; however, the powder pattern we calculated from this single-crystal data [14b] does not match the experimental pattern (see Fig. 2, top and middle) obtained for our CaIn_2S_4 whiskers. Care was taken to avoid preferred orientation in obtaining the diffraction pattern of our CaIn_2S_4 whiskers, but, as a precaution, a Gandoifi pattern of several crystals was used to confirm the absence of the strong low-angle lines apparent in the pattern calculated from the single-crystal data reported for $\text{Ca}_{3.1}\text{In}_{6.6}\text{S}_{13}$ [14b]. These differences in the powder patterns (Fig. 2) and stoichiometries of $\text{Ca}_{3.1}\text{In}_{6.6}\text{S}_{13}$ and the CaIn_2S_4 whiskers indicate that the CaIn_2S_4 whiskers are a new compound. $\text{Ca}_{3.1}\text{In}_{6.6}\text{S}_{13}$ reportedly exhibits partial occupancy of calcium sites and also substitution of calcium into indium sites [14b]; thus, its structure may allow a variation in cation stoichiometry. The similar unit cells obtained for CaIn_2S_4 and $\text{Ca}_{3.1}\text{In}_{6.6}\text{S}_{13}$ indicate the possibility of very similar structures. Unfortunately, the CaIn_2S_4 whiskers obtained in the present study were not sufficiently crystalline for a full single-crystal structure determination. Further crystal growth experiments are in progress.

The color, stoichiometry, and X-ray powder pattern of the bronze $\text{Ca}_{1.2}\text{In}_{1.9}\text{S}_4$ whiskers (Fig. 2, bottom) do not match those of the previously discussed compounds. $\text{Ca}_{1.2}\text{In}_{1.9}\text{S}_4$ appears to be another new compound in the Ca-In-S ternary system. The whiskers were insufficiently crystalline and singular for an unambiguous unit cell to be determined using single-crystal methods. The best of four crystals appeared to be split, but a primitive monoclinic cell was found after removal of reflections from one of the halves. The other crystals gave differing C-centered monoclinic cells, but the axial photographs did not agree with the cells. None of the cells could account for all of the powder X-ray diffraction data from a sample of crushed whiskers. 42 of the 46 observed reflections could be indexed on the primitive monoclinic cell mentioned above: $a = 14.642(4)$, $b = 3.865(1)$, $c = 29.60(1)$ Å, and $\beta = 97.84(2)^\circ$. The unindexed lines were consistent with one or more of the C-centered cells mentioned above. A number of polytypes could be possible and crystal growth experiments are in progress to obtain whiskers suitable for crystal structure determination.

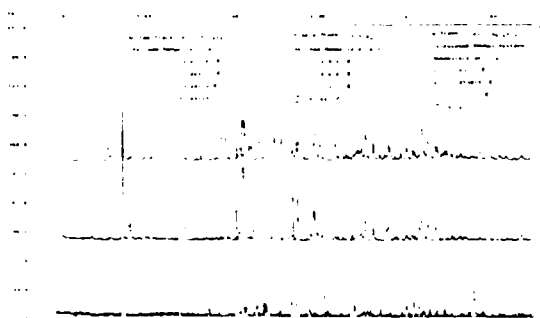


Fig. 2. X-ray powder patterns of (top) $\text{Ca}_{3.1}\text{In}_{6.6}\text{S}_{13}$ (calculated); (middle) CaIn_2S_4 ; and (bottom) $\text{Ca}_{1.2}\text{In}_{1.9}\text{S}_4$.

$\text{Sr}_{0.9}\text{In}_{2.1}\text{S}_4$ grew as yellow whiskers similar in size, color, and morphology to the CaIn_2S_4 whiskers. The X-ray powder pattern (Fig. 3, bottom) shows a structure very different from that reported for SrIn_2S_4 [15], which is the only previously reported ternary strontium indium sulfide. The pattern shown for SrIn_2S_4 in Fig. 3 (top) was calculated using atomic positions reported for isostructural BaIn_2S_4 [16] with the SrIn_2S_4 cell parameters [15]. Unit cell determination of a single crystal of $\text{Sr}_{0.9}\text{In}_{2.1}\text{S}_4$ indicated a C-centered monoclinic cell. All powder diffraction data from the crushed crystals could be indexed on this cell: $a = 27.66(1)$, $b = 3.943(2)$, $c = 12.683(7)$ Å, $\beta = 94.25(4)^\circ$. The whiskers were insufficiently crystalline for a single crystal structure determination. Further crystal growth experiments are in progress.

The polycrystalline BaIn_2S_4 that we prepared gave an X-ray powder diffraction pattern in good agreement with that calculated from the reported crystal structure [16], as shown in Fig. 4. All data were indexed using an orthorhombic unit cell ($a = 21.852(4)$, $b = 21.744(5)$, $c = 13.125(4)$ Å) that is consistent with the literature report.

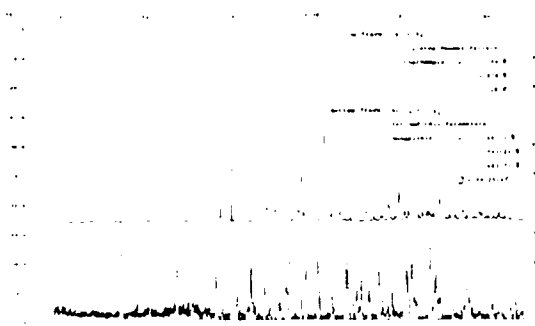


Fig. 3. X-ray powder patterns of (top) SrIn_2S_4 (calculated); and (bottom) $\text{Sr}_{0.9}\text{In}_{2.1}\text{S}_4$.

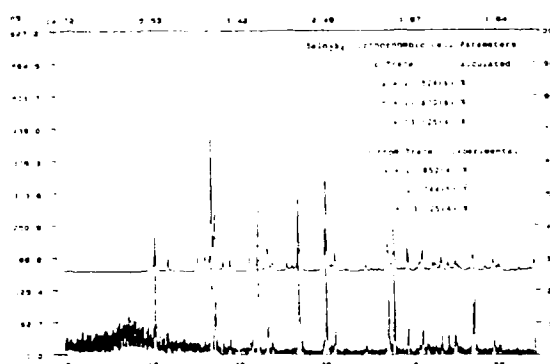


Fig. 4. X-ray powder patterns of BaIn_2S_4 (top) calculated; and (bottom) experimental.

TGA plots of powdered whiskers of CaIn_2S_4 and $\text{Ca}_{1.2}\text{In}_{1.9}\text{S}_4$ under flowing O_2 are shown in Fig. 5. CaIn_2S_4 begins to decompose at about 350°C and $\text{Ca}_{1.2}\text{In}_{1.9}\text{S}_4$ begins to decompose at about 425°C .

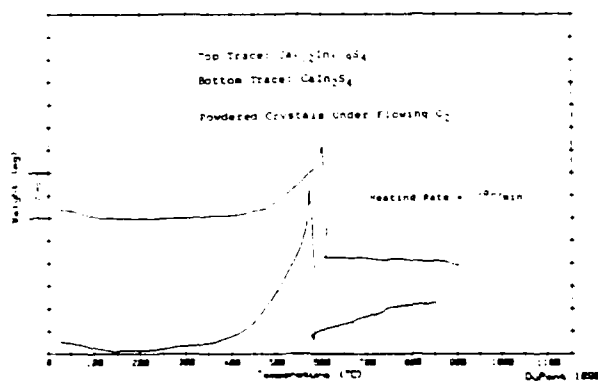


Fig. 5. TGA of (top) $\text{Ca}_{1.2}\text{In}_{1.9}\text{S}_4$; and (bottom) CaIn_2S_4

The infrared (diffuse reflectance) spectra of CaIn_2S_4 , $\text{Ca}_{1.2}\text{In}_{1.9}$, and $\text{Sr}_{0.9}\text{In}_{2.1}\text{S}_4$ are shown in Fig. 6. All three compounds show strong decreases in transmission in the 700-

750 cm^{-1} (13-14 μm) range. Absorption bands above 750 cm^{-1} arise from impurities, notably CO_3^{2-} (711, 875, 1397, 1622, and 1795 cm^{-1} for CaCO_3). The broad band at 1070 cm^{-1} indicates the presence of sulfate, which may also increase the frequency of the IR transmission loss above the intrinsic values of the sulfides. Diffuse reflectance is more sensitive to surface impurities than transmission measurements, but the crystals were too small for true single-crystal transmission measurements.

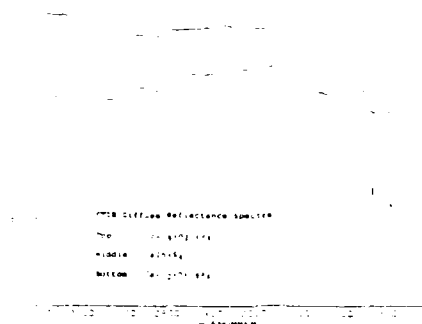


Fig. 6. FTIR Diffuse Reflectance Spectra of (Top) $\text{Sr}_{0.9}\text{In}_{2.1}\text{S}_4$; (Middle) CaIn_2S_4 ; and (Bottom) $\text{Ca}_{1.2}\text{In}_{1.9}\text{S}_4$.

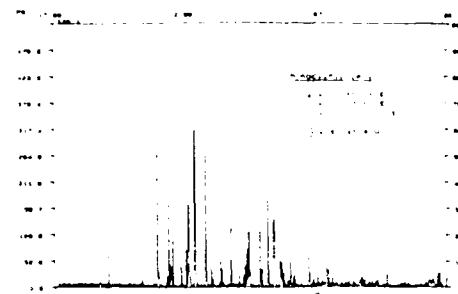


Fig. 7. X-Ray Powder Diffraction Pattern of CaY_2S_4 .

CaY_2S_4 System

The X-ray diffraction pattern of polycrystalline CaY_2S_4 is shown in Fig. 7. The data could not be completely indexed on the basis of either of the reported orthorhombic unit cells given in Table I. All reflections could be indexed, however, using a monoclinic cell: $a = 12.95(1)$, $b = 13.03(1)$, $c = 3.957(2)$ Å; $\beta = 93.45(5)^\circ$. This result is in good agreement with the reported monoclinic cell given in Table I. Unfortunately, the CaY_2S_4 whiskers obtained in the crystal growth experiment were poorly crystalline and single-crystal data could not be obtained. Further experiments are in progress to obtain good crystals for a full structure determination.

The X-ray powder diffraction patterns for the $\text{Ca}_5\text{Y}_2\text{S}_8$ crystals with (top trace) and without (bottom trace) added commercial CaS are shown in Fig. 8; both samples contained NBS silicon as an internal standard. The shrinkage of the CaS lattice due to incorporation of the smaller Y^{3+} ion is clearly seen by comparing the top and bottom traces in Fig. 8. The F-centered cubic cell parameters obtained were: CaS, $a = 5.6945(5)$ Å; $\text{Ca}_5\text{Y}_2\text{S}_8$, $a = 5.6646(3)$ Å, indicating a volume decrease of about 2% upon substitution of 0.375 mol (Y^{3+} plus vacancies) in the CaS lattice. A Vegard's Law-type plot for the system is shown in Fig. 9. The predicted cell edge for full substitution of Ca^{2+} by Y^{3+} based on relative ionic sizes alone [23] and neglecting electroneutrality is plotted on one extreme with the observed value for CaS on the other. The observed cell edge for $\text{Ca}_5\text{Y}_2\text{S}_8$, in which 1/4 of the cation sites in the CaS lattice are occupied by Y^{3+} and 1/8 are vacant, is indicated on the plot. The observed cell edge is greater than that expected for hypothetical $\text{Ca}_5\text{Y}_2\text{S}_8$, hence the "size" of the vacancy seems to be greater than a Ca^{2+} ion. The crystal volume appears to be somewhat expanded; this could be attributable to bond-weakening effects of cation vacancies.

Single-crystal X-ray diffraction data obtained for one of the $\text{Ca}_5\text{Y}_2\text{S}_8$ crystals confirmed the unit cell indicated by the powder data; no indication of a superstructure could be observed, indicating apparent disorder of the Ca^{2+} , Y^{3+} , and cation vacancies in a simple rock-salt-type lattice. Further crystal growth experiments with modified cooling rates are in progress to obtain ordered crystals.

The thermogravimetric curves for CaY_2S_4 , $\text{Ca}_5\text{Y}_2\text{S}_8$, and CaS under oxygen are shown in Fig. 10. All of the compounds commence decomposition between 450-500°C; however, the rates of decomposition are significantly different.

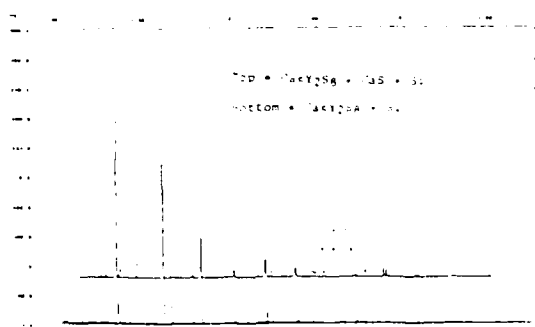


Fig. 8. X-ray Powder Diffraction Patterns of $\text{Ca}_5\text{Y}_2\text{S}_8$ crushed crystals (Top) with and (Bottom) without added CaS. Both samples contain NBS standard silicon; the CaS contains CaO impurity.

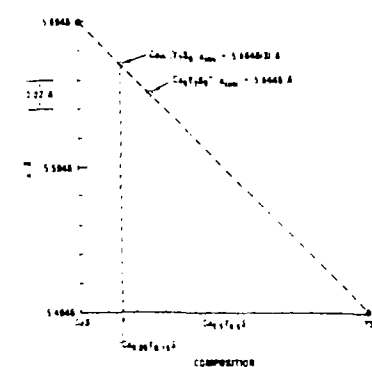


Fig. 9. Vegari's Law-type plot for Y^{3+} substitution in CaS.

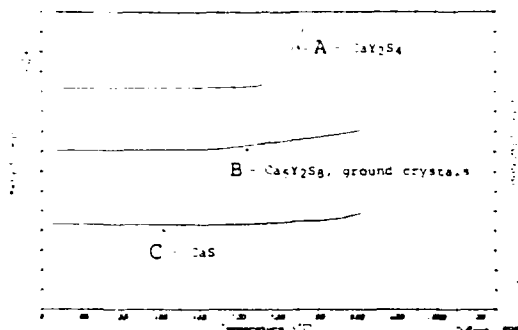


Fig. 10. TGA profiles for (A) CaY_2S_4 , (B) $\text{Ca}_5\text{Y}_2\text{S}_8$, and (C) CaS; all were obtained under flowing oxygen.

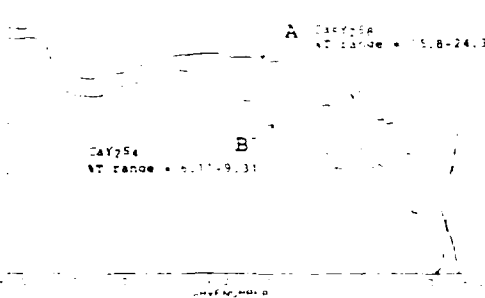


Fig. 11. Transmission IR spectra of (A) a $\text{Ca}_5\text{Y}_2\text{S}_8$ crystal (approx. 0.6 mm thick) and (B) a mat of CaY_2S_4 whiskers; the y-axis ranges for the two spectra are different: A: %T = 15.8-24.3 B: %T = 6.11-9.31

Transmission infrared spectra of a mat of the CaY_2S_4 whiskers and an approximately 0.6 mm thick $\text{Ca}_5\text{Y}_2\text{S}_8$ crystal are shown in Fig. 11. In both spectra, absorption bands above 600 cm^{-1} are attributable to oxide impurities, particularly outstanding in the spectrum of the CaY_2S_4 whisker-mat (B) because of the very long effective pathlength. In the spectrum of the $\text{Ca}_5\text{Y}_2\text{S}_8$ crystal (A), a strong decrease in infrared transmission commences near $10\text{ }\mu\text{m}$. Spectrum B of the CaY_2S_4 whiskers shows no such decrease down to 450 cm^{-1} , in agreement with the studies on powder samples [20].

ACKNOWLEDGEMENTS

We are grateful to Dr. M.P. Nadler for the infrared studies. We thank Mike Hasting and Dan Bliss for the thermal analyses, Rudy Muro for the ICP measurements, Bob Woolever and Rick Schen for the SEM/EDX analyses, and Laurie Zellmer for assistance in obtaining the X-ray powder diffraction data.

This work was supported by the Office of Naval Research. D.O.K. is grateful to the American Society for Engineering Education for a postdoctoral fellowship.

REFERENCES

1. G.A. Slack in Advanced Materials for Optical Windows, G. E. Technical Information Series No. 79CRD071, June 1979.
2. S. Musikant, R.A. Tanzilli, R.J. Charles, G.A. Slack, W. White, and R.M. Cannon in Advanced Optical Ceramics, Phase I, G. E. Document No. 78SDR2195, May 1978.
3. R.M. Hazen and L.W. Finger, in Comparative Crystal Chemistry, (John Wiley & Sons, New York, 1982), p. 136.
4. O. Muller, in Crystal Chemical Data for Ternary Chalcogenide and Polysulfide Compounds, Scientific Report No. 1, Air Force Contract No. F19628-71-C-0232, August 1972.
5. N.R. Kyle, R.R. Stephens, M.E. Pedinoff, S.R. Sashital, A.L. Gentile, and J.F. Lotspeich, in Development of New Electro-Optic and Acousto-Optic Materials, Air Force Technical Report RADC-TR-83-243, November 1983.
6. C.E. Johnson, T.A. Vanderah, C.G. Bauch, and D.C. Harris, Proc. SPIE 968, 41 (1988).
7. H. Hahn, G. Frank, W. Klingler, A. Stoerger, and G. Stoerger, Z.anorg. allg. Chem. 272, 241 (1955).
8. J.M. Zhang, W.W. Chen, B. Dunn, and A.J. Ardell, Proc. of the SPIE 968, (1988).
9. A. Wold (private communication), 1988.
10. R. Nitsche, H.U. Boeisterli, and M. Lichtensteiger, J. Phys. Chem. Solids 21, 109 (1961).
11. J.A. Beun, R. Nitsche, and M. Lichtensteiger, Physica 27, 448 (1961).
12. B. Vengatesan, N. Kanniah, and P. Ramasamy, Phys. Stat. Sol. 104, K93 (1987).
13. H. Hahn and W. Klingler, Z. anorg. allg. Chem. 263, 177 (1950).
- 14a. G. Chapuis, A. Niggli, and R. Nitsche, Naturwissenschaften 58, 94 (1971).
- b. G. Chapuis and A. Niggli, J. Solid State Chem. 5, 126 (1972).
15. P.C. Donohue and J.E. Hanlon, J. Electrochem. Soc. 121, 137 (1974).
16. B. Eisenmann, M. Jakowski, W. Klee, and H. Schafer, Rev. Chim. Miner. 20, 255 (1983).
17. J. Flahaut, L. Domange, and M. Patne, Bull. Soc. Chim. 1, 105 (1961).
18. M. Patne and J. Flahaut, C.R. Acad. Sc. Paris 264, 395 (1967).
19. H.L. Tsai and P.J. Meschter, J. Electrochem. Soc. 128, 2229 (1981).
20. H.L. Park, C.A. Chess, and W.B. White in The Rare Earths in Modern Science and Technology, G.J. McCarthy, J.J. Rhyne, and H.B. Silber, Eds.; Plenum Press, N.Y.: 1980, p. 451-6.
21. Alfred S. Gates, Jr., Ph.D. Dissertation, The University of Toledo, 1976.
22. W.B. White in Advanced Optical Ceramics, Phase II, GE Report for ONR Contract N00014-78-C-0466, DIN:80SDR2172, August 1980.
23. R.D. Shannon, Acta Crystallogr. A32, 751 (1976).